이학석사 학위논문

Photo-initiated Polymerization of Hydrogel by Graphene Quntum Dots

그래핀 양자점을 이용한 하이드로겔 광촉매 중합 및 특성 연구

2016년 8월

서울대학교 대학원
화학부 물리화학 전공
김 유 나

Abstract

Photo-initiated Polymerization of Hydrogel by Graphene Quantum Dots

Yuna Kim

Department of Chemistry

Seoul National University

As a smart stimulus material, hydrogel attracts significant attention in various fields of application and research for drug delivery, actuators and sensors, and in tissue engineering. The mechanical properties and the three-dimensional porous network of hydrogels, highly dependent on the polymerization process of its components, can be modulated with introduction of different nanoparticles. Among which, we have examined that graphene quantum dot (GQDs) itself can effectively participate in photo polymerization process of acrylamide hydrogel as the photo catalyst.

The GQDs exhibit unique photoelectric effects among any other forms of graphene. Thus, the hydroxyl radicals generated by photo catalytic effect of GQDs participate in polymerization of hydrogel by initiating double bonds in the gel solution to form monomer radicals for further polymer network. The photo

polymerization by GQDs suggests a simple polymerization process for hydrogels with even under sunlight and a controllable gelation rate by manipulating the concentration of GQDs. The gelation process of hydrogel due to photo catalytic effect in this work is analyzed by using the dynamic light scattering (DLS) measurement and its network structures are seen by SEM and TEM images. Additionally, upon enforcing ionic bond and introducing nanoparticles within the system, the mechanical behavior of hydrogels is significantly enhanced; analyzed by compressive and tensile strength tests.

The GQDs in the hydrogel system shows synergetic effect not only in polymerization as a photo catalyst for monomer crosslinking but also in increasing the mechanical strength of intrinsically weak hydrogel; allowing for a wide range of promising applications in the future.

Keywords: Graphene Quantum Dots, Hydrogels, Photo catalysis, Polymerization, Organic–inorganic Nanostructure

Student Number: 2014–21230

Table of Contents

List of Figures

(black) and retract (red) a) AGel b) GQDGel_0.1 c) GQDGel_0.2 d) GQDGel_0.4 e) Adhesion force and mean standard deviation obtained from 22 measurements for each sample.

Figure 5. a) Photograph of heat press tester machine. b) Hydrogel test samples prepared for the test (left: AGel and right: GQDGel_0.4) on 1 cm grid square. Photograph of hydrogel sample between the two plates of the tester c) AGel and d) GQDGel_0.4. Photograph of hydrogel after 5 Psi. compression load for e) AGel and f) GQDGel_0.4.

Figure 6. Scanning electron microscopy images of GQDGel_0.1 polymerization process from a) 0 min, no irradiation, b) 5 min, c) 15 min, d) and 30 min of irradiation under the sunlight.

Figure 7. SEM image and structure of AAm to MBaa ratio 40:1 of hydrogels a) AGel, b) GQDGel_0.2, and c) GQDGel_0.4. For AAm to MBaa ratio 400:1 fabricated hydrogels d) AGel, e) GQDGel_0.2, and f) GQDGel_0.4.

Figure 8. Transmission electron microscopy images of the GQDGel_0.1 sample after polymerization.

Figure 9. Dynamic light scattering time−intensity correlation functions of a) Agel b) GQDGel_0.1 and c) GQDGel_0.2 samples during irradiation under sunlight for different times. Normalized

structure factor of a) Agel b) GQDGel_0.1 and c) GQDGel_0.2 samples. g) Heterodyne parameter (Y) as a function of polymerization time. h) Plot of Gelation factor(k) as a function of time.

Figure 10. a) Swelling ratio measurement to increase in time from 0 min. to 1260 min. b) Exponential curve fitting of swelling ratio shows ampliture of 1209 for AGel and 234 for GQDGel. c) Average of maximum swelling ratio and and mean standard deviation obtained from three measurements for each sample. d) Photograph of hydrogel swelling process from dry to swollen in DI water of Agel, GQDGel_0.1, GQDGel_0.2, GQDGel_0.4, GQDGel_1 from left to right respectively.

Introduction

1.1 Introduction

The hydrogel is known for its various significant behaviors such as being temperature, pH, and chemical sensitive and for its functional structural behaviors.[1,2] The three-dimensional porous structural network of hydrogels highly depend on the polymerization process and the ratio of its monomer and crosslink components. Also, known to be highly biocompatible, usage of hydrogel in the medical industry have been rapidly evolving.[3] Yet some of the limitations of hydrogels are that its intrinsic mechanical behavior is known to be very brittle showing low stretch-ability and compression strength. Thus, fabrication of highly elastic hydrogel[4,5] has been a challenge and various methods has been proposed to synthesize hydrogels with different nanoparticles.[6] Such hybridization of nanostructured hydrogel or promoting ionic crosslinks into the structure have shown to enhance the mechanical and sensitive behaviors of intrinsic hydrogels.[7,8]

In this research, we examined GQDs as the photo catalyst for polymerization of polyacrylamide hydrogel. The graphene quantum dots (GQDs), among any other different forms of graphene, are known to have distinct photoactive properties such as being fluorescent due to quantum confinement and edge site significant features. Aside from photoactive effects,GQDs also establish favorable condition for hydrogel polymer composite

process considering high water solubility, biocompatible, and edge functional properties of GQDs. Laboratory synthesized GQDs not only show broad absorption in the visible spectrum from 400 to 700 nm but can also serve as smart photosensitizers with under visible-light irradiation (≥420 nm) suitable for reactions under visible, sunlight and UV light. Therefor, developing an effective method to produce hydrogel from visible-light-active GQDs as photocatalysis via energy transfer mechanism is hightly appealing. As a metal-free nano-particle, GQDs compared to other forms of semiconductor nanoparticles such as TiO2 or ZnO,[9] is a more convincing alternate material as photo catalyst especially for bio compatible applications of the hydrogel such as in drug delivery,[10] and tissue engineering.[11]

Experimental Section

2.1 Hydrogel Perparation

We have synthesized GQDs photo-initiated hydrogel(GQDGel) by first preparing a gelatin aqueous solution of acrylamide (AAm) and N,N-methylenenbisacrylamide (MBaa) dissolved in deionized water. GQDs were added in place of a photo initiator. A controlled concentration of GQDs were used; the value 0.1, 0.2, 0.4, and 1 ml followed by GQDGel represents the amount of GQDs solution used per 3 ml of gelatin solution. These values indicate 0.0013, 0.0027, 0.0054, and 0.012 wt% GQDs respectively. A typically used photo-initiator, ammonium persulphate (APS), was used for a different batch of gel aqueous solution for comparison (AGel). After degassing each solution in a vacuum chamber for 30 min each, N,N,N,N' -tetramthylethylene (TEMED) was added as catalysis. As prepared solution was put under sunlight or UV for polymerization in glass vial. The same GQDs based gel solution was kept in a dark room for 24 hours and showed no indication of polymerization as shown in Figure 1c. The significant reaction of our recipe was that the sunlight excited GQDs provided enough initiation of radical generation for polymerization as a replacement of a typical photo-initiator. The free radicals are easily inhibited by the reduction of water molecules in an aqueous solution.[12] The nanoparticles should have a moderate bandgap, which is easy to be excited by sunlight to form active

radicals.

Macromolecular network is the basic structure of a hydrogel, which is covalent cross-link or physically entangled. The polyacrylamide hydrogel undergoes polymerization of alkene (C=C) group in vinyl monomers into a chain.[13] Polymers are made from free radical polymerization process where the initiators such as APS for this specific experiment exhibit free radicals when a pair of electrons separate as the bonds break. Then, these unpaired electrons attack the carbon-carbon double bond and react with the acrylamide monomers. As formed monomer molecules grow in chains as the unpaired electrons propagate. Such process progressed until the reaction eventually comes to termination as the radicals find a pair or by molecule coupling.[14] The APS in the reaction is a strong oxidizing agent as a source of sulfate ester radicals. Only a controlled amount of APS is used in various commercial products such as in bleaching because of its harmful effects on bronchus, skin, and asthmatic effects upon exposure to high level of dosage is not negligible.[15] Therefore, replacement of APS with bio friendly and convenient photo-initiator is promising for polyacrylamide hydrogel polymerization.

2.2 Graphene Quantum Dots (GQDs) synthesis

Considering such vinyl polymerization process of acrylamide hydrogel and some of the harmful effect of APS or other sulfuric acids, GQDs are expected to behave as a sufficient

photo initiator in polymerization. The GQDs were synthesized by chemical oxidation process following the method reported by Peng *et al.*.[16] As shown in Figure 2a, the size of as-fabricated GQDs range from 0.5 to 2 nm indicating a few layers of graphene. The photoluminescence excitation and emission spectra in Figure 2b show two sharp PLE peaks at 330 nm and 429 nm and PL peak at 318 nm of yellow GQDs. The Fourier transform infrared (FTIR) spectrum in Figure 2c show oxygen containing groups in GQDs; including carboxylic acid, ester, and aromatic ether groups. These functional groups are also responsible for highly water soluble GQDs which will be further analyzed from swelling. Also, the enhanced oxidative sites on GQDs accounts for increased generation of hydroxyl radicals. Therefore, highly oxidized GQDs are more favorable as a photo initiator.

In order for photochemical reaction to occur with GQDs as the photo initiator, following aspects are required[17]: 1) GQDs must be a photosensitive molecule with an absorption wavelength range adequate for initiation of reaction, 2) absorbed photon must have sufficient energy to excite GQD particles to exert free radicals, 3) functional groups account for an efficient reaction. GQDs have been notified for their excellent photo luminescent properties behaving as both electron donors and acceptors.[18] Graphene quantum dots (GQDs) in the reaction behaves as a photo catalyst and exert hydroxyl radicals as depicted in below when irradiated:

$$Reduction: O_2 + e^- \rightarrow O_2^- \quad (1)$$

$$Oxydation: H_2O \text{ or } OH^- + h^+ \rightarrow \bullet OH + H^- \quad (2)$$

The hydroxyl radicals account for initiation of acrylamide vinyl monomer polymerization as the radicals attack the polyacrylamide and yield main-chain scission. The reaction does not account for graphene oxides. The GQDs synthesized with visible light is irradiated at 429 nm and various source of light such as visible light, sunlight, ultraviolet (UV) lamp, or laser can be used to cure hydrogel from aqueous solution to gel.

Results

3.1 Mechanical strength

One of the main limitations of hydrogel is that they have a very poor mechanical property considering a substantial fraction of hydrogel materials is water. The brittle materialistic properties of hydrogel have been engineered and hybrid multicomponent materials have been developed to build robust hydrogel networks.[19] In terms of determining the physical properties of gels, the most important distinction is understanding the chemically bonded networks between polymers and those of between polymer chains. Such physical entanglements are analyzed from various mechanical strength test measurements. In this research, tensile force, surface adhesion energy, and compression tests were driven for GQDGels and AGel. The ability to fabricate extremely robust hydrogel hybrids contributes to enhance the application possibility of hydrogel such as, electronic devices robustly embedded with tough hydrogel or utilization in soft robotics and actuator applications.

3.1.1 Tensile test

The tensile strength of typical hydrogel depends on the cross-linker (MBaa) component. The tensile strength measurement is the force required to pull a significant material. The Young's modulus can be calculated from the slope of the

strain versus stress measured from tensile tests. The movement of the polymer chains in hydrogel are molecularly restricted or mobilized by the amount of crosslinks, limiting the stretchable behavior of polymer chains. The GQDs induced hydrogels exhibit high toughness and relaxed movement of the polymers increasing linear flexibility. The hydrogel samples prepared are in a dog bone shape from lab fabricated polydimethylsiloxane (PDMS) mold as shown in Figure 5c with a display of hydrogel sample clamped on the tensile testing machine. The hydrogel samples were stretched from 2.0 cm to 3.3cm. From the measurement, the results show that the AGels have higher Young' s modulus for increased AAm to MBaa ratio. Also, as for GQDGel, the maximum Young' s modulus measured was 540 kPa with hydrogel aqueous solution of AAm to MBaa ratio of 40:1 for GQDGel_0.4. The measured Young' s modulus of GQDGel was 50 times larger than the measurement of intrinsic AGel and enhanced measurements are expected with increased GQD concentration and MBaa.

3.1.2 Surface adhesion energy

Atomic force microscope (AFM) can be used to measure the surface forces and adhesion energy of materials in atomic level. The measurement of the AFM is used to measure the mechanical contact force, van der Waals forces, capillary forces, and chemical bonding.[20] The force displacement measurement from contact mode AFM was used to obtain surface adhesion for each hydrogel samples. The adhesion energy of a material is defined as the free energy change to separate unit areas of two media from contact to infinity. The pull-off force during

retraction of the AFM tips give information about the amount of free chemical chains on the surface of hydrogel.[21]

The intrinsic properties of hydrogel has also low surface adhesion, and introduction of nanoparticles can driving polymer adsorption.[22] The measured surface adhesion force of GQDGel not only showed strengthened crosslinking structure of the hydrogel but also enhance the adhesion of the hydrogel surfaces which is highly restrained. Hydrogel with high surface adhesion and viscosity can be obtained with GQDs. The outermost layer of each surface plays a crucial role in adhesive properties, and amount of interdigitating accounts for increased van der Waals bonds. As shown from the mapping of the force–displacement measurement, the average of maximum surface adhesion force of GQDGel was 1.0310^{-4} Nm compared to 4.1110^{-5} Nm for AGel. It is also observable fom the measured tip approach and retract plot that the adhesion force is maintained for a steadier distance using retraction. Obtaining high surface energy hydrogel accounts for possible applications in microfluidic systems to sustain high flow rates, high pressure and large deformation undergoing physiological environments.

3.1.3 Compression test

Among many applications of hydrogel, cartilage repair strategy is one of the notorious application of hydrogel.[23] Yet, in order to replace damaged cartilage tissue with hydrogel, its compression modulus is significant in providing appropriate stiffness and deformation properties are important in fracture resistance.[24] The compression test is considered as the most straight forward evaluation of measuring the toughness of

hydrogels. The compression properties are tested to assess the mechanical properties of GQDs reinforced hydrogels in comparison to intrinsically brittle AGel. The pressure applied to the surface of the hydrogel and distance of compression can be used to calculated the mechanical properties of hydrogel. For this specific experiment, the compression test was carried out by placing each hydrogel specimen between two plates and compressing it with controlled load of 6 psi as shown in Figure 5. Each sample was 2.3 cm in diameter and 1cm thick. The results show that AGel under compression strength could not withhold the force and broke into pieces while for GQDGels_0.4, the hydrogel maintained its shape and was free of damage or cracks. Failure of material due to compression comes from fracture points of the macromolecules. The enhanced compression pressure resistance of the GQDGel indicates flexibility of the molecular bonds due to more contact sites of the polymer and cross-linker bonds.

3.2 Hydrogel Structure

A unique three-dimensional porous structure can be observed from SEM images of hydrogel.[25] The cross-sectional view of freeze-dried and 30nm Pt coated AGel and GQDGel samples show highly porous structure with its pore sizes ranging from several ones to tens of micrometers. The SEM images were observed in chronological order to see the change in the structure as the polymerization proceeds. The analyzed images show reaching out and initiated monomers to bond with one another and with crosslinks. As the irritation process, the

polymerization becomes thicker and forms the porous structure. The walls of the polymers become smooth as the polymerization comes to termination and no more active sites are left for reaction.

The synthesized hydrogel pore sizes depend on the ratio of monomer (AAm) to cross-linker (MBaa), as shown in Figure 6a-d. As the ratio of monomer to cross-linker increases, the pore size of the hydrogel decreases. The GQDs initiated hydrogels are expected to have a similar porous structure as that of typical hydrogel and the pore sizes seem to be fairly uniform across the interior as a consequence of stable polymerization process. The "wall" of the polymer forming the pores seems to be thicker for increased concentration of GQDs; the images compared from Figure 7a and c to Figure 7d and f. The TEM analysis reveals that the GQDs are randomly dispersed and embedded within the polymer crosslinks (Figure 8a-f). From overall observation of the TEM images, the GQDs seem to be fairly aggregated and bonded with the polymer bonds. The GQDs embedded and bonded with the hydrogel are also expected affect the mechanical properties of the hydrogel.

Discussion

4.1 Dynamic Light Scattering

As a result of a dynamic light scattering (DLS) experiment, the phase relations of the light scattered by different particles change randomly and also the number of particles in the scattering volume fluctuates.[26,27] Because the Brownian motion or diffusion of the particles in the suspension is the cause of the fluctuations, information about the diffusion process can be obtained from an analysis of the intensity fluctuations in terms of a time correlation function. The measurement of DLS is the normalized intensity-time autocorrelation (IFC) function, given by:

$$g_2(\tau) = \frac{< I(q,0)I(q,\tau) >}{< I(q,0) >^2} \qquad (3)$$

where τ is the decay time, is the average scattering intensity at τ, and q is scattering wave vector. The DLS measurements can provide useful information about the polymerization process of GQDs induced sol to gel transition. For instance, the measurements show that slow mode diverges and power-law behavior appears at the sol-gel transition. The intensity of the gel can be considered as the sum of fluctuating component(I_F)

and static component (I_C).

There has been a few reports previously on the usage of DLS measurements to understand the polymerization process of hydrogels. DLS spectrum of hydrogel solution(sol) is known to have a distinguishable investigation for when it is in the gel phase; also distinguishable for when the samples are at sol phase, a sol−gel transition phase, and at gel phase. Yet, it has been only recently in 2013, that Asai *et al.* was the first to use DLS to evaluate the dynamics during gelation process to understanding synthesis information of tough ion−gels.[28] The heterodyne parameter (Y) in Figure 4d has been evaluated from the approach reported by Asai *et al.*. Additionally, in 2016, Kumar *et al.* have proposed a parameter called the Gelation factor (κ),[29] obtained from the dynamic structure factor data to show a trend of transition from solution to gel states.

$$\kappa = 1 - \left| \frac{S_{Et}(q,0) - S_{Et}(q,\infty)}{S_{Et=0}(q,0) - S_{Et=0}(q,\infty)} \right| \qquad (4)$$

Polymerization behavior of gelatin aqueous solutions can be investigated using the dynamic light scattering(DLS) measurements. For a polymeric gel, cross−linked polymers are less capable of diffusion and interdigitation as the molecules are bonded together. Therefore, the information of DLS of decreased decay time and diffusion can be used to analyze the polymerization process of gels. For our purposes, DLS has been measured in respect of increase of time the sample was exposed

to sunlight in increments of 5 min. Response rate of polymerization due to photo initiator is proportional to the amount of GQDs were proportional to the amount of GQDs in the gel solution. Higher component of GQDs in the hydrogel exhibited faster gelation process compared to that of less amount of GQDs. The GQDGel polymerization has an average decay time of 20 to 40 min until the polymerization process comes to complete termination.

4.2 Swelling

The cross-linked polymer hydrogels swell when water or solvent enters.[30] The swelling properties, which usually use degree of swelling is analyzed to define hydrogels, depend on many factors such as network density, solvent nature, polymer solvent interaction parameter, and the pore size of hydrogel which is controlled by the density of cross-linker reagents. The high water affinity of GQDs due to the many oxide sites on GQDs account for faster swelling rate of the hydrogel compared to Agel. The swelling rate (Q) of the hydrogel can be measure by the following equation:

$$Q = \frac{W_s - W_d}{W_d} \times 100\% \quad (5)$$

where W_s is the weight of swollen hydrogel at time t and W_d is the weigh of the dry hydrogel at t=0. The plotted swelling rate for AGel and GQDGel are shown in Figure 8a. The exponential fitted slope also shows a faster swelling rate of GQDGel up to

six times the AGel. Also, the water content of hydrogels can be calculated after the equilibrium swelling by:

$$Water\,content = \frac{W_{s_{eq}}}{W_d} \times 100\% \qquad (6)$$

The result of the water content measured is shown in Figure 8c. The results show that GQDGel have higher water content for GQDGel_0.1 and GQDGel_0.2 than AGel. However, when the excess amount of GQDs participate in the polymerization such as for GQDGel_0.1 the GQDs particles merge out from the porous hydrogel link and the final swollen weight of the hydrogel is less than that of the AGel. Another cause of decrease in swelling due to increasing concentration of GQDs is because the mean distance between the network nodes shrink. Yet a controlled amount of GQDs yields increased water content of hydrogel compared to its intrinsic properties. The amount of water content for hydrogel thus can be suggested not only to have been increased but also to be modulated with the amount of GQDs.

Methods

Synthesis of polyacrylamide hydrogel

The materials and suppliers used for acrylamide hydrogel were acrylamide monomer (AAm; Sigma, A8887), N,N−methylenebisacrylamide (MBaa; Sigma, M7279), ammonium persulfate (APS; Sigma, A9164), and N,N,N,N−tetramethylethylenediamine(TEMED; Sigma, T7024) as crosslinking accelerator. AAM and MBaa were dissolved in deionized (DI) water with AAm at 2 M and amount of AAm to MBaa weight ratio of 40:1 or 400:1. After degassing in a vacuum chamber, TEMED 0.003 the weight of AAm and APS 0.002 weight of AAm was added. The solutions were poured in a cylinder glass vial size of 1550 mm unless otherwise stated in the paper. The APS gels were cured using ultraviolet light for at least 20 min.

Synthesis of graphene quantum dots

Carbon fiber were added into a mixture of concentrated H_2SO_4 and HNO_3 in 3:1 ratio. The mixed solution was sonicated for two hours and stirred for 24 hours at 120° C. The mixture was cooled and diluted with deionized water and the PH was adjusted to 8 by adding Na_2Co_3. The final product was then further dialyzed in a dialysis bag for 3 days.

GQDs characterization

The GQD layers were characterized using various microscopic and spectroscopic techniques. The surface micrographs and images were obtained using an atomic force microscope (AFM) in noncontact mode (XE-100, Park System). FTIR spectra were obtained on a Nicolet FTIR. The photoluminescence characterization was done using a luminescence spectrometer (HORIBA) with xenon lamp as the source of excitation.

GQDGel prepolymer preparation and polymer synthesis

AAm and MBaa were dissolved in deionized water with 40 to 1 ratio. The solution was degassed in a vacuum chamber for in average 30 min until in equilibrium. As prepared solution was used as a base solution for fabrication of both APS and GQDs based hydrogel synthesis. TEMED was fixed for 20ml for all conditions. Synthesized GQDs solvent were mixed with deionized water in 0.01 g to 15 ml to be proportionately used for hydrogel synthesis. The GQDs based gels were cured under sunlight in a 50 ml vial.

Polymerization Dynamic Light Scattering

The gel mixture in solution was poured in DLS cuvettes 1 ml and the cuvettes were put out in the sunlight for GQDs polymerization. The measurement was carried out with Zetasizer Nano at 25° C and scattering angle of 275° .

Mechanical Properties of GQDsGel and hybrid hydrogels

For tensile strength test, a universal testing systems (INSTRON 5948, Microtester) was used. A dog-bone shape of hydrogel specimen is favored for measurement polymer or hydrogel materials. Some PDMS molds in shape of a dog-bone 2.0 x 0.2 cm was fabricated. Hydrogel mixture solution was poured into the fabricated PDMS mold and left under the sunlight for polymerization. The fabricated hydrogel specimens underwent load measuring tensile strength test and its extension speed was set at 2 mm per min.

For compression test, hydrogel sample was prepared from a vial and each specimen in volume of. Heating press tester (QM900, QMesys) was used to observe and compared the change in the hydrogel after undergoing a compression load of 6 psi. The movements of the hydrogels were recorded using a DSLR camera (Cannon).

The atomic force microscope (XE-100, Park System) was used to measure the surface adhesion energy of the hydrogel. The adhesion energy value displayed is the average of the values measure from contact-mode force versus displacement mapping measurement.

SEM and TEM of hydrogels

For scanning electron microscopy observation, each sample underwent freeze-drying process. Frozen in liquid nitrogen for 5 min. and dried in low temperature vacuum for 24 hrs. The dried AGel and GQDsGel were cut to smaller pieces

and 40 nm of Pt coated for SEM imaging. Field-Emission scanning electron microscope (SIGMA) was used with operating voltage of 10 kV.

For TEM sampling, thin layer of hydrogel was polymerized directly on TEM copper grid and dried in ambient condition for 4 days. The Cs corrected TEM with Cold FEG (JEM-ARM200F) was used with operating voltage of 80 kV.

Conclusion

6.1 Conclusion

In Summary, we have synthesized and characterized a new nano-composite hydrogels using GQDs as its photo-initiating reactant. Introducing unique photochemical properties, GQDs inhibit efficient crosslinking process of acrylamide monomers enhancing its mechanical strength and swelling properties. The gelation process of hydrogel due to photo catalytic effect in this work is analyzed by using the dynamic light scattering measurement and its network structures were observed by SEM and TEM images. Additionally, upon enforcing ionic bond and introducing nanoparticles within the system, the mechanical behavior of hydrogels is significantly enhanced; analyzed by tensile strength, surface adhesion, and compressive tests. GQDs based polyacrylamide gels with characteristic network and fluorescent properties may be useful for understanding the network of polymers and in applications such as biomedical tissue engineering, drug delivery systems, and mechanical devices.

7. Bibliography

1. Keplinger, C.; Sun, J.-Y.; Foo, C. C.; Rothemund, P.; Whitesides, G. M.; Suo, Z., Stretchable, transparent, ionic conductors. *Science* 2013, *341* (6149), 984-987.

2. N. A. Peppas; Y. Huang; M. Torres-Lugo; J. H. Ward, a.; Zhang, J., Physicochemical Foundations and Structural Design of Hydrogels in Medicine and Biology. *Annual Review of Biomedical Engineering* 2000, *2* (1), 9-29.

3. Chung, K.; Wallace, J.; Kim, S.-Y.; Kalyanasundaram, S.; Andalman, A. S.; Davidson, T. J.; Mirzabekov, J. J.; Zalocusky, K. A.; Mattis, J.; Denisin, A. K., Structural and molecular interrogation of intact biological systems. *Nature* 2013, *497* (7449), 332-337.

4. Gong, J. P.; Katsuyama, Y.; Kurokawa, T.; Osada, Y., Double-network hydrogels with extremely high mechanical strength. *Advanced Materials* 2003, *15* (14), 1155-1158.

5. Okumura, Y.; Ito, K., The polyrotaxane gel: A topological gel by figure-of-eight cross-links. *Advanced Materials* 2001, *13* (7), 485-487.

6. Xia, L.-W.; Xie, R.; Ju, X.-J.; Wang, W.; Chen, Q.; Chu, L.-Y., Nano-structured smart hydrogels with rapid response and high elasticity. *Nat Commun* 2013, *4*.

7. Zhang, D.; Yang, J.; Bao, S.; Wu, Q.; Wang, Q., Semiconductor nanoparticle-based hydrogels prepared via self-initiated polymerization under sunlight, even visible light.

Scientific Reports 2013, *3*, 1399.

8. Haraguchi, K.; Takehisa, T., Nanocomposite hydrogels: a unique organic–inorganic network structure with extraordinary mechanical, optical, and swelling/de–swelling properties. *Advanced Materials* 2002, *14* (16), 1120.

9. Huang, Z.–Y.; Barber, T.; Mills, G.; Morris, M.–B., Heterogeneous photopolymerization of methyl methacrylate initiated by small ZnO particles. *The Journal of Physical Chemistry* 1994, *98* (48), 12746–12752.

10. Rosiak, J.; Burozak, K.; Pękala, W., Polyacrylamide hydrogels as sustained release drug delivery dressing materials. *Radiation Physics and Chemistry (1977)* 1983, *22* (3), 907–915.

11. Christensen, L. H.; Breiting, V. B.; Aasted, A.; J ϕ rgensen, A.; Kebuladze, I., Long–term effects of polyacrylamide hydrogel on human breast tissue. *Plastic and reconstructive surgery* 2003, *111* (6), 1883–1890.

12. Stroyuk, A.; Granchak, V.; Korzhak, A.; Kuchmii, S. Y., Photoinitiation of buthylmethacrylate polymerization by colloidal semiconductor nanoparticles. *Journal of Photochemistry and Photobiology A: Chemistry* 2004, *162* (2), 339–351.

13. Bamford, C. H., *The kinetics of vinyl polymerization by radical mechanisms*. Academic Press: 1958.

14. Mino, G.; Kaizerman, S., A new method for the preparation of graft copolymers. Polymerization initiated by ceric ion redox systems. *Journal of Polymer Science* 1958, *31* (122), 242–243.

15. Janney, M. A.; Omatete, O. O.; Walls, C. A.; Nunn, S. D.;

Ogle, R. J.; Westmoreland, G., Development of low-toxicity gelcasting systems. *Journal of the American Ceramic Society* 1998, *81* (3), 581-591.

16. Peng, J.; Gao, W.; Gupta, B. K.; Liu, Z.; Romero-Aburto, R.; Ge, L.; Song, L.; Alemany, L. B.; Zhan, X.; Gao, G., Graphene quantum dots derived from carbon fibers. *Nano letters* 2012, *12* (2), 844-849.

17. Chatani, S.; Kloxin, C. J.; Bowman, C. N., The power of light in polymer science: photochemical processes to manipulate polymer formation, structure, and properties. *Polymer Chemistry* 2014, *5* (7), 2187-2201.

18. Wang, X.; Cao, L.; Lu, F.; Meziani, M. J.; Li, H.; Qi, G.; Zhou, B.; Harruff, B. A.; Kermarrec, F.; Sun, Y.-P., Photoinduced electron transfers with carbon dots. *Chemical Communications* 2009, (25), 3774-3776.

19. Anseth, K. S.; Bowman, C. N.; Brannon-Peppas, L., Mechanical properties of hydrogels and their experimental determination. *Biomaterials* 1996, *17* (17), 1647-1657.

20. Ng, S. S.; Li, C.; Chan, V., Experimental and numerical determination of cellular traction force on polymeric hydrogels. *Interface Focus* 2011, *1* (5), 777-791.

21. Ahadian, S.; Ram□n-Azc□n, J.; Estili, M.; Liang, X.; Ostrovidov, S.; Shiku, H.; Ramalingam, M.; Nakajima, K.; Sakka, Y.; Bae, H., Hybrid hydrogels containing vertically aligned carbon nanotubes with anisotropic electrical conductivity for muscle myofiber fabrication. *Scientific reports* 2014, *4*.

22. Rose, S.; Prevoteau, A.; Elzi□re, P.; Hourdet, D.;

Marcellan, A.; Leibler, L., Nanoparticle solutions as adhesives for gels and biological tissues. *Nature* 2014, *505* (7483), 382-385.

23. Lee, S.-Y.; Pereira, B. P.; Yusof, N.; Selvaratnam, L.; Yu, Z.; Abbas, A.; Kamarul, T., Unconfined compression properties of a porous poly (vinyl alcohol)-chitosan-based hydrogel after hydration. *Acta biomaterialia* 2009, *5* (6), 1919-1925.

24. Xiao, Y.; Friis, E. A.; Gehrke, S. H.; Detamore, M. S., Mechanical testing of hydrogels in cartilage tissue engineering: beyond the compressive modulus. *Tissue Engineering Part B: Reviews* 2013, *19* (5), 403-412.

25. Kim, S. H.; Chu, C. C., Synthesis and characterization of dextran-methacrylate hydrogels and structural study by SEM. *Journal of biomedical materials research* 2000, *49* (4), 517-527.

26. Okamoto, M.; Norisuye, T.; Shibayama, M., Time-resolved dynamic light scattering study on gelation and gel-melting processes of gelatin gels. *Macromolecules* 2001, *34* (24), 8496-8502.

27. Matsunaga, T.; Shibayama, M., Gel point determination of gelatin hydrogels by dynamic light scattering and rheological measurements. *Physical Review E* 2007, *76* (3), 030401.

28. Asai, H.; Nishi, K.; Hiroi, T.; Fujii, K.; Sakai, T.; Shibayama, M., Gelation process of Tetra-PEG ion-gel investigated by time-resolved dynamic light scattering. *Polymer* 2013, *54* (3), 1160-1166.

29. Kumar, N.; Kumar, V.; Sharma, J., Relaxations in gelatin hydrogels probed by dynamic light scattering.

30. Ganji, F.; Vasheghani-Farahani, S.; Vasheghani-Farahani,

E., Theoretical description of hydrogel swelling: a review. *Iran Polym J* 2010, *19* (5), 375-398.

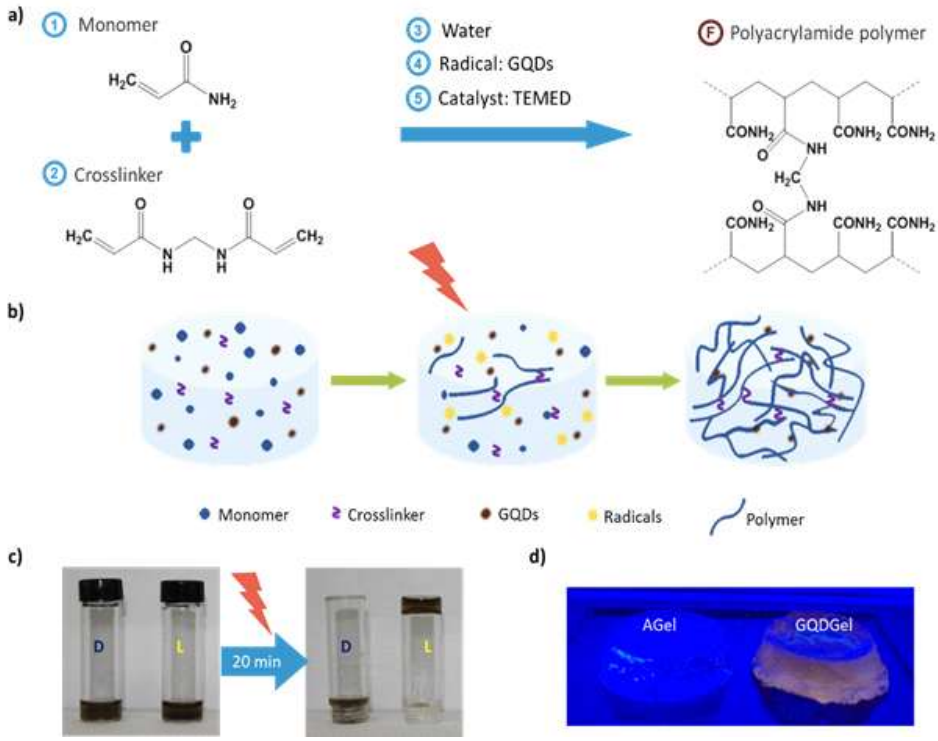

Figure 1. a) Molecular structure and precursor solution containing GQDs to develop final product of polyacrylamide polymer. b) Schematics of polymerization process of hydrogel from solution state to radical excitation to polymer. c) Photographs of prepared hydrogel polymerized under sunlight for 20 min. compared to non-polymerized solution in darkroom for 24 hrs. (D: darkroom and L: sunlight) d) Indication of fluorescent GQDGel in UV 365nm compared to none fluorescent AGel.

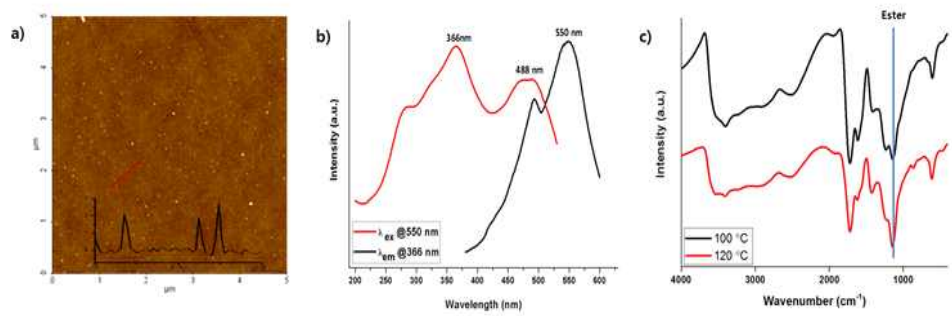

Figure 2. a) AFM image of GQDs. b) Photoluminescence spectrum of GQDs with emission at 550 nm and excited at 366 nm c) FTIR spectra of GQDs for 100 ° C and 120 ° C.

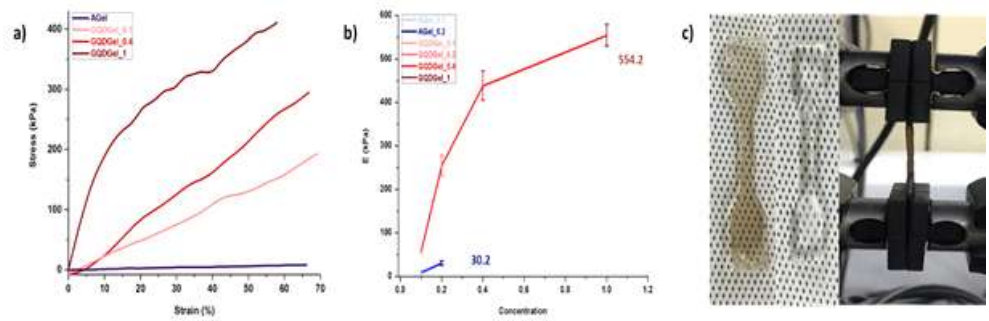

Figure 3. a) Stress vs strain measurement from tensile test b) Measured Young's modulus for AGel and GQDGel. c) Photograph of dog bone shaped hydrogel specimen fabricated (left) and during the tensile testing process (right).

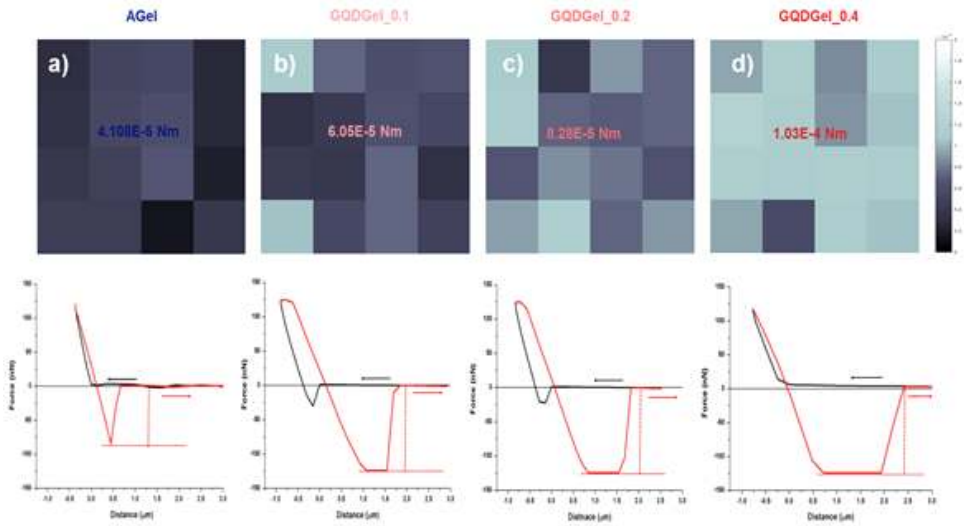

Figure 4. Mechanical properties of AGel and GQDGel measured by contact mode AFM measurement. Right: Adhesion force map of hydrogel samples dimension 10 □m x 10 □m. Number in the middle is the average of the adhesion force measured from mapping. Left: Force deformation curve of cantilever approach (black) and retract (red) a) AGel b) GQDGel_0.1 c) GQDGel_0.2 d) GQDGel_0.4

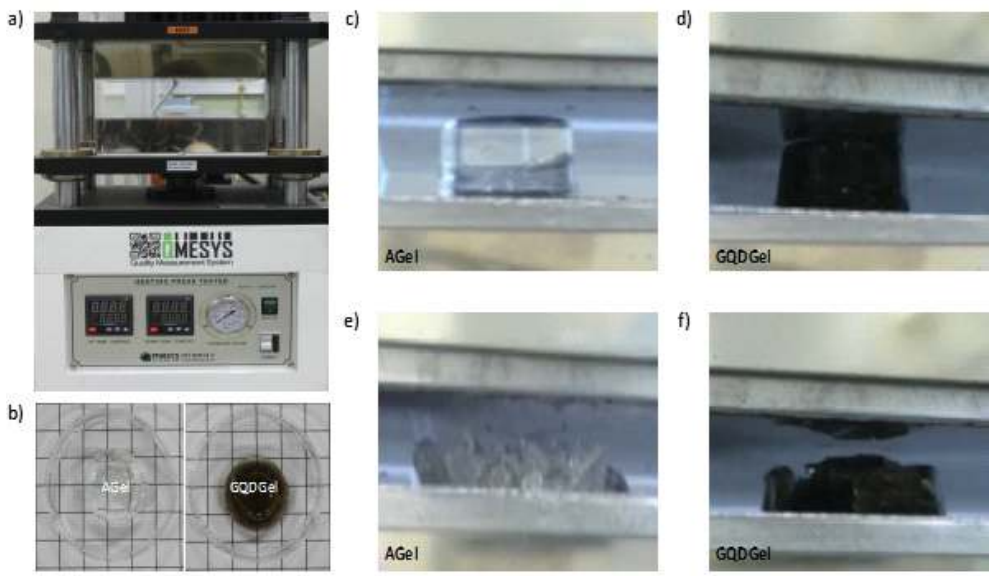

Figure 5. a) Photograph of heat press tester machine. b) Hydrogel test samples prepared for the test (left: AGel and right: GQDGel_0.4) on 1 cm grid square. Photograph of hydrogel sample between the two plates of the tester c) AGel and d) GQDGel_0.4. Photograph of hydrogel after 5 Psi. compression load for e) AGel and f) GQDGel_0.4.

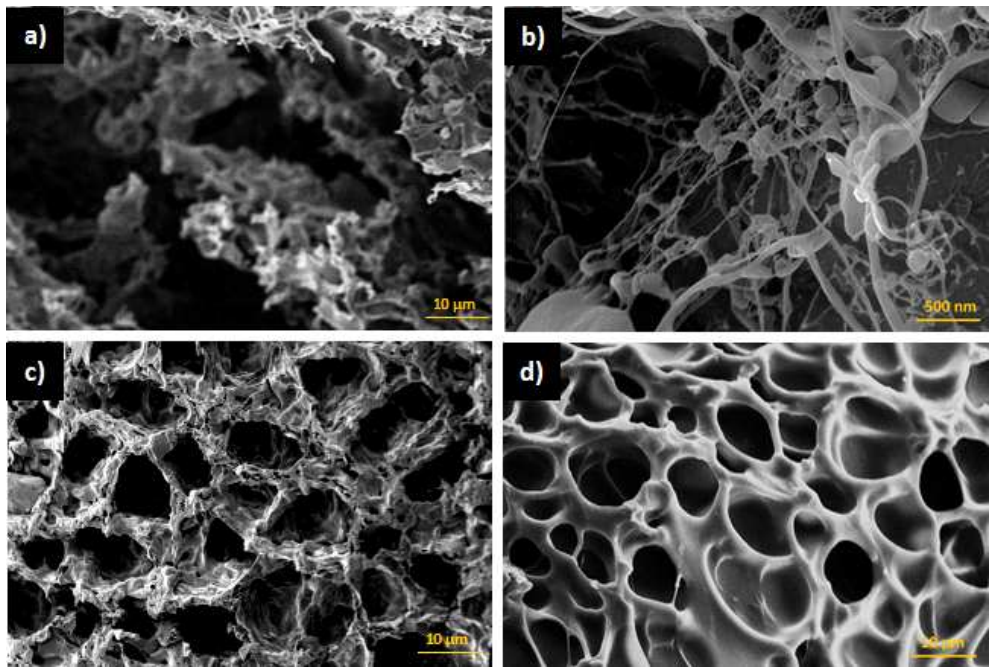

Figure 6. Scanning electron microscopy images of GQDGel_0.1 polymerization process at a) 0 min, no irradiation, b) 5 min, c) 15 min, d) and 30 min of irradiation under the sunlight.

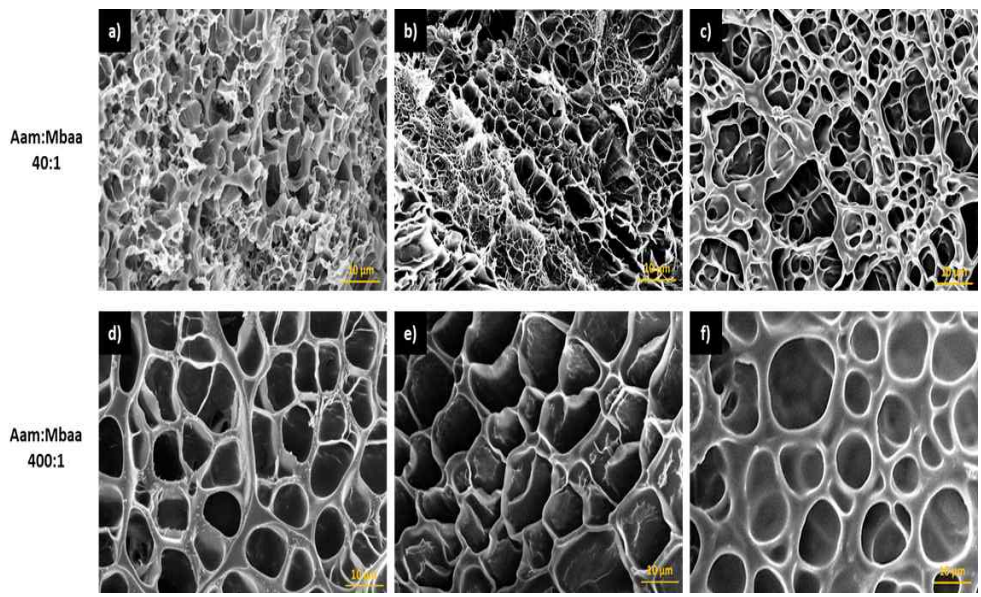

Figure 7. SEM image and structure of AAm to MBaa ratio 40:1 of hydrogels a) AGel, b) GQDGel_0.2, and c) GQDGel_0.4. For AAm to MBaa ratio 400:1 fabricated hydrogels d) AGel, e) GQDGel_0.2, and f) GQDGel_0.4.

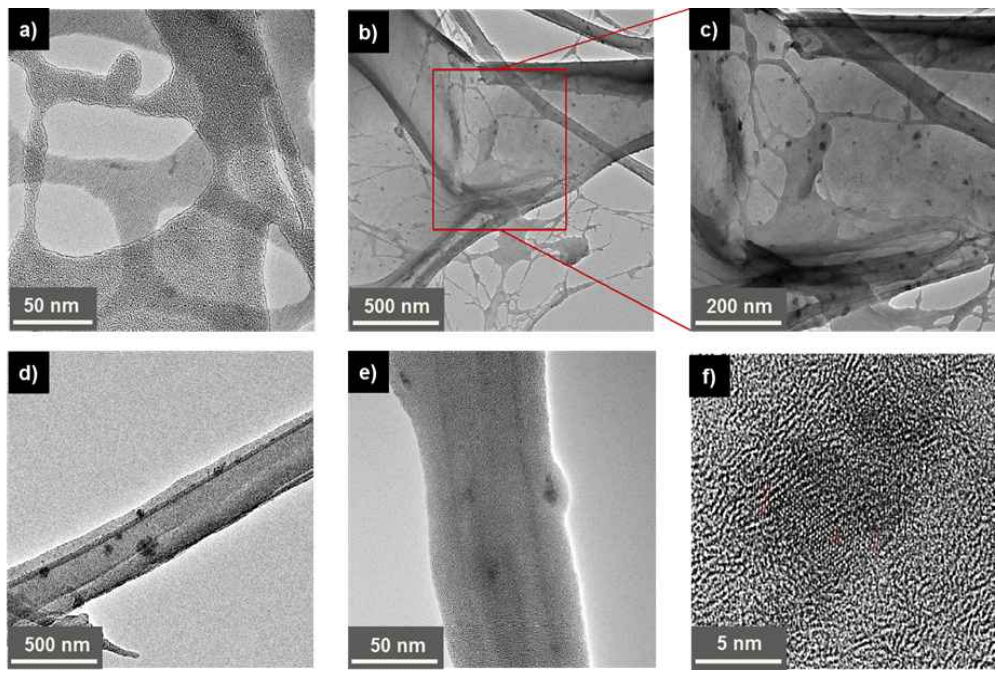

Figure 8. Transmission electron microscopy images of the GQDGel_0.1 sample after polymerization.

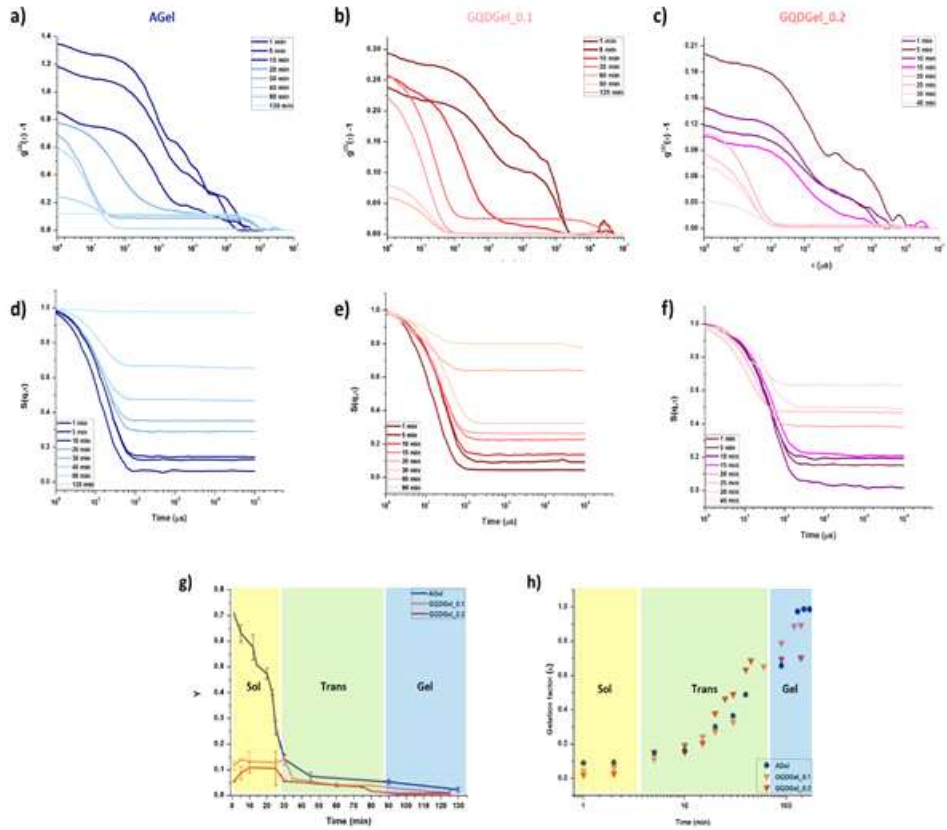

Figure 9. Dynamic light scattering time−intensity correlation functions of a) Agel b) GQDGel_0.1 and c) GQDGel_0.2 samples during irradiation under sunlight for different times. Normalized structure factor of a) Agel b) GQDGel_0.1 and c) GQDGel_0.2 samples. g) Heterodyne parameter (Y) as a function of polymerization time. h) Plot of Gelation factor(k) as a function of time.

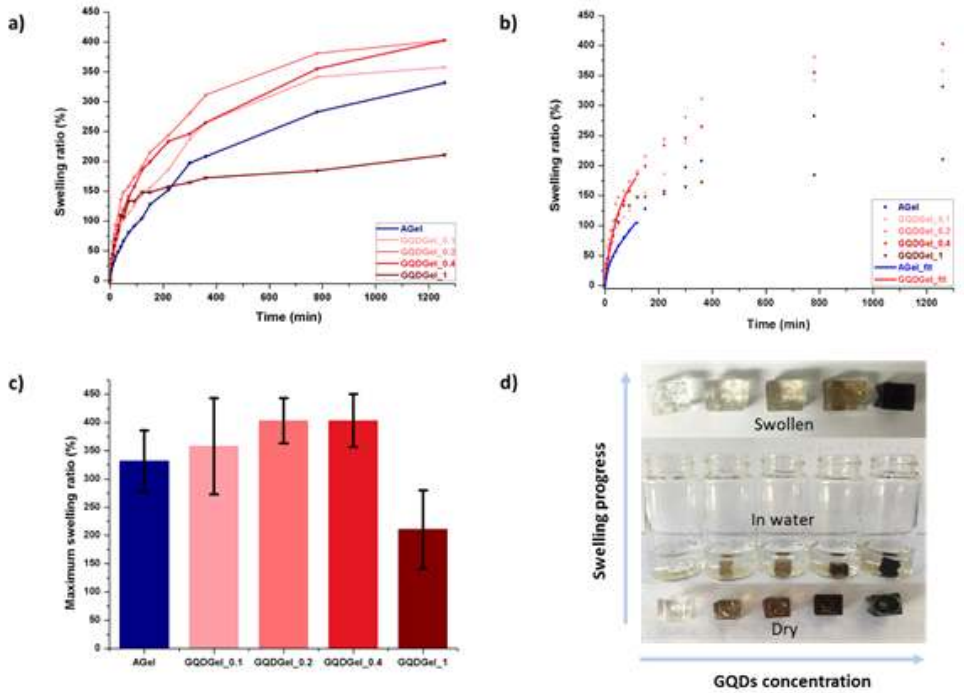

Figure 10. a) Swelling ratio measurement to increase in time from 0 min. to 1260 min. b) Exponential curve fitting of swelling ratio shows ampliture of 1209 for AGel and 234 for GQDGel. c) Average of maximum swelling ratio and and mean standard deviation obtained from three measurements for each sample. d) Photograph of hydrogel swelling process from dry to swollen in DI water of Agel, GQDGel_0.1, GQDGel_0.2, GQDGel_0.4, and GQDGel_1 from left to right respectively.

국문초록

그래핀 양자점을 이용한 하이드로겔 광촉매 중합 및 특성 연구

김 유 나
화학부 물리화학 전공
서울대학교 대학원

하이드로겔은 매우 높은 수분 함유량을 갖고 산소 투과성이 높은 물질로서 치료 목적, 조직세포 재생과 같은 생물학적 응용부터 로보틱스, 센서, 전도도를 활용한 응용까지 그 활용범위가 넓어 많은 분야의 연구자들에게 실험되어지고 있고 사용범위 역시 증가하고 있다. 본 실험은 그래핀 양자점을 하이드로겔의 광촉매로 사용하여 그에 따른 하이드로겔 분석 및 신체사용에도 무해한 나노물질 하이드로겔을 소개한다.

폴리아크릴아마이드 하이드로겔는 라디컬에 의한 중합과정을 갖는데, 일반적인 광황산염 라디칼 의유도 촉매인 APS 가 아닌 그래핀 양자점을 광촉매로 사용한 새로운 방법의 고분자 중합과정을 분석하였다. 그래핀 양자점은 그래핀의 다양한 형태 중에서도 유일한 광화학의 특성을 지니며 빛의 조사에 의해서 하이드록시기 라디칼을 생성하는 산화과정을 지니게 된다. 발광에 의해 생성된 라디컬이 아크릴아마이드 단위체 결합에 적극적으로 참여하여 고분자의 중합을 유도하게 되는 것이다. 제조한 나노복합체는 TEM, SEM, DLS, UV-vis 분광기를 이용하여 그 형태, 다공성, 사이즈 분포 및 광학적 특성을 분석하였고, 인장, 응착력, 응압힘에 의한 하이드로겔의 기기적 하이드로겔의 기기적 특성을 분석하였다. 이러한 합성기법은 하이드로겔의 향상된 기기적 특성과 안정적이고 접근에 용이한 중합 방법을 제시하며 다양한 응용에도 적합하여 유용

하게 사용될 수 있다.

Keywords: 그래핀 양자점, 하이드로겔, 광촉매, 고분자 중합, 나노구조

학번: 2014-21230